

Identification of Acid-soluble Components and Acid-insoluble Inclusions in Spark OES Pulse-height Distribution Analysis

Kazumi MIZUKAMI*
Wataru OHASHI
Masaharu TSUJI

Masaaki SUGIYAMA
Kaoru MIZUNO

Abstract

The spark OES-PDA (Pulse height Distribution Analysis) method has been widely used in the field of steel making processes, as a rapid composition analysis of elements, such as aluminum in molten steel, according to the chemical states respectively: acid soluble (Sol.), insoluble(Insol.) and the Total (Insol.+Sol.). When a sample surface is sparked, several thousands of elemental emission intensities are stored and transformed to the frequency distribution of PDA histogram. In literature, symmetric normal distribution of low intensity pulses on the histogram was identified to be the acid soluble (Sol.) component in the metal, whereas the high intensity pulses were attributed to the acid insoluble inclusions (Insol.). In this study, the collapse process of inclusions on the sample surface was investigated using optical microscope, SEM-EDS, EPMA, and spark-OES. It was found that the number of inclusions decreased sharply before the stable discharge region over 500 pulses, because the inclusions were initially destroyed and dispersed finely into the metal matrix. As the result, the emission intensities of the symmetric normal distribution region are superimposed on those of finely dispersed inclusions (Fine insol.) and the elements dissolved in the metal (Sol.). It is proposed in this study that symmetric normal distribution of the PDA histogram should be reassigned to the Total (Insol.+Sol.).

1. Introduction

In steel production, the contents of carbon and other alloying elements in steel are controlled during the refining process of the steel making plant, and it is very important for producing steels of excellent quality in great quantities repetitively to enhance the process control function so that the chemistry and temperature of molten steel

in the furnace are controlled to be within their respective target ranges in a limited time. Spark source optical emission spectrochemical analysis (spark-OES, also widely known as QuantVAC (QV)), is capable of rapidly and accurately quantifying different component elements in steel samples taken from refining processes, allowing rapid feedback of the determination results to the operation people, and for this reason, it is used in many metal melting factories world-

* Chief Researcher, D.Eng., Materials Characterization Research Lab., Advanced Technology Research Laboratories 20-1, Shintomi, Futsu, Chiba

wide.

By this method, several thousands of electrical discharge sparks are formed per second between a specimen and a counter electrode; emission lines, which are unique to different elements, emitted by the spark are detected using a photoelectric multiplier or the like, and the elements that cause them are identified based on the wavelengths of the lines. At the same time, the amount of each element is determined based on the optical emission intensity and by referring to the working curve of the element. In addition, through digital conversion of the emission intensity data, the pulse-by-pulse method, and statistical processing of the digitized data, it is possible to determine the quantities and the states of specific elements such as Al, Ti, and B, that is, how much of each element is in solute form in the steel and how much is in the form of non-metallic inclusions (hereinafter referred to simply as inclusions).

Generally, component elements in solute form in steel can be considered soluble in acid (acid-soluble, hereinafter simply referred to as soluble, or "Sol."), and are effective in improving steel properties such as toughness, ductility, magnetic properties, etc. On the other hand, when they form compounds insoluble in acid (acid-insoluble, hereinafter simply referred to as insoluble, or "Insol."), they form large inclusions adversely affecting product quality (surface defects, failure of wire under tension, etc.). A paper was publicized in 1974 reporting that the pulse-height distribution analysis (PDA) method was effective in quickly identifying and determining the amounts of Sol. and Insol. in steel, and ever since, many researchers have studied this method.¹⁻⁸⁾

It has been more than 30 years since vacuum spark-OES devices equipped with the PDA function began to be used for process control in the steel industry, and yet today, they continue to serve as quick, accurate, and reliable analysis instruments; this method is used in metal refining industries all over the world in preference to other instrumental analysis techniques. In addition, various improvements for quickly determining the composition and size distribution of inclusions have been developed and applied to equipment to further enhance its usefulness.^{9, 10)}

Whereas the amount of Sol. determined by the conventional PDA method agrees well with that determined by chemical analysis as far as commercially produced steels are concerned, it has been known through experience that the two values do not agree with each other in the case, for example, of steels containing large amounts of insoluble Al such as those for shop tests. Although various measures to minimize this deviation have been proposed,^{11, 12)} the cause of the deviation resulting from an increase in the content of insoluble Al relative to total Al has not been clarified. On the other hand, to meet the need to improve the target hitting performance in the steel refining process, especially in the production of high-grade and high-purity steels over the last few years, it is necessary to re-establish theories for quickly and accurately determining Al, Ti, and other deoxidizing agents in different states over wider ranges of concentration and to develop such determination methods.

To point out problems of the determination method based on conventional PDA theory and to develop a basic concept for determining different states of alloy elements in molten metal more accurately and over wider concentration ranges, the authors examined the breakdown processes of inclusions in the elementary reactions of optical emission in spark-OES. As a result of clarifying the chronological change in the shape, number, and composition of inclusions over the period from the time when a spark discharge begins to hit inclusions in steel up to the stage of stable discharge, the authors

found that some points in the assignment practice according to conventional PDA theory had to be corrected, and consequently proposed a new assignment method.

2. Experimental Methods and Materials

Fig. 1 schematically illustrates the type PDA-5500 atomic emission spectrometer manufactured by Shimadzu Corporation that the authors used in the present test. The concave diffraction grating of the device has a curvature radius of 600 mm and 2400 grooves every 1 mm. The operation conditions were as follows: a tungsten counter electrode; discharging voltage, 500 V; frequency, 333 Hz; Ar gas flow, 12 l/min; and Ar flashing, 5 s. Argon gas of 99.999% purity was cleaned by passing it through a column filled with molecular sieves. The analytical lines were Al I 396.1 nm and Ti II 332.7 nm. As the Fe internal standard lines, Fe II 271.4 nm was used for Al, and Fe I 287.2 nm was used for Ti. Several thousands of normal sparks were formed between the counter electrode and a specimen set in the analysis apparatus. The optical emission intensity of each element during each pulse was measured employing time-resolved PDA photometry. A scanning electron microscope, S-4000 of Hitachi Ltd., and an electron probe micro-analyzer (EPMA) for two-dimensional mapping, JXA-8900RL manufactured by JEOL, were used for structural observation.

3. Test Results

3.1 Test on the relationship between Sol. and Insol. and PDA mode

According to the conventional theory of spark-OES, the optical emission intensity during each pulse is statistically processed, plotted on a PDA histogram where the abscissa represents the emission intensity and where the ordinate represents the frequency of incidence, and optical emissions forming a normal distribution pattern on the low-intensity side are assigned to Sol., and those distributed on the high-intensity side are assigned to Insol. To confirm whether the above assignment was true for specimens having different contents of the element in question, the authors conducted the following tests.

Table 1 shows the chemical compositions of the specimens used for the present test; they were pure iron, JSS reference samples, and a Ti sample specially prepared using a vacuum melting furnace. The table also shows the mode values of the normal distribution patterns on the low-intensity side of their respective PDA histograms. The

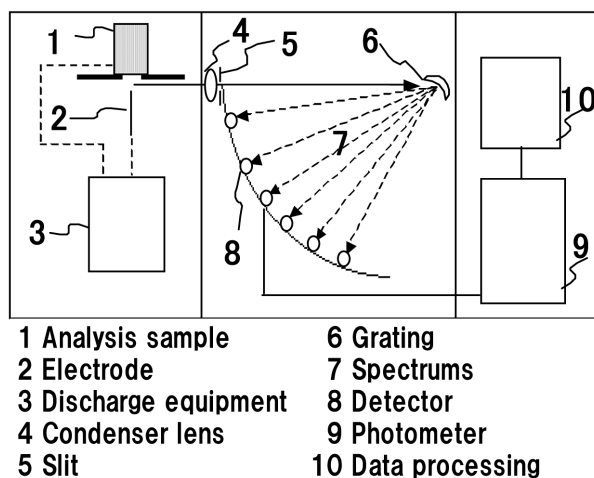
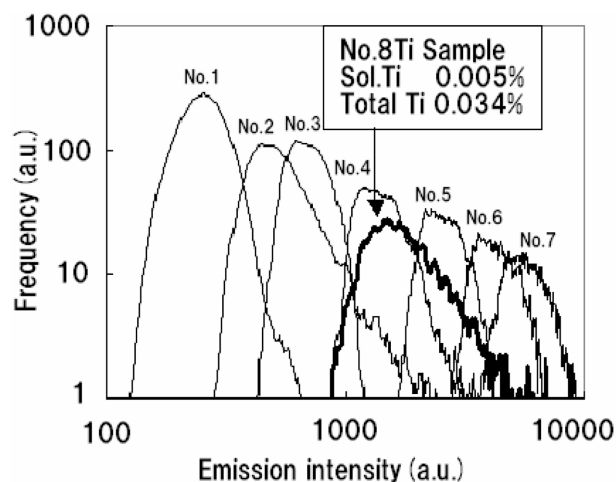


Fig. 1 Spark-OES experimental setup

Table 1 Chemical compositions and PDA mode value of samples

No.	1	2	3	4	5	6	7	8
Sample name	Pure iron	JSS 1006-1	JSS 1004-1	JSS 1007-1	JSS 171-6	JSS 168-6	JSS 170-6	Ti sample
Total Ti (wt%)	0.000	0.005	0.009	0.021	0.046	0.078	0.103	0.034
Sol.Ti (wt%)	0.000	0.001	0.003	0.015	0.007	0.008	0.009	0.005
Insol.Ti (wt%)	0.000	0.004	0.006	0.006	0.040	0.070	0.094	0.029
Mode (a.u.)	260	470	650	1230	2370	3810	4970	1700



No.1 (Total Ti: 0.000%), No.2 (0.005%), No.3 (0.009%), No.4 (0.021%), No.5 (0.046%), No.6 (0.078%), No.7 (0.103%), No.8 (0.034%)

Fig. 2 Corresponding PDA graphs of Ti taken from sample No.1 to 8 listed in Table 1

chemical analysis figures for the soluble and insoluble Ti were obtained by collecting grinding chip samples of the specimens, dissolving them through low-temperature heating in a (1 + 6) sulfuric acid solution, screening the solution with 5C filter paper, melting the residue, and then subjecting the residue to spectrophotometry with diantipyryl methane. As a pre-treatment for the spark-OES analysis to prepare the PDA histograms, the specimen surfaces were polished by belt grinding to 100 mesh. After a pre-discharge of 1000 pulses of normal sparks and 4000 pulses of analyzing sparks (twice 2000 each), the pulse intensities of all the component elements were fed to the data processor, and the intensities of Ti in all the samples over the 4000 pulses of analyzing discharge were converted into PDA histograms.

Fig. 2 shows the PDA histograms of the samples with respect to Ti; here, the abscissa represents the emission intensity and the ordinate represents the frequency of incidence, both in logarithmic scale. The specimens were those listed in Table 1. As seen here, the curves shifted to the high-intensity side as the Ti content increased. The bold curve of the graph shows the analysis result of the Ti sample (sample No. 8 of Table 1, containing 0.034% total Ti and 0.005% soluble Ti) specially prepared for the present test; the normal distribution curve of this specimen has a mode between 0.021 and 0.046% Ti. According to the conventional PDA method of assignment, whereby optical emissions in a normal distribution pattern on the low-intensity side are assigned to Sol., the curve of the Ti sample should have appeared more to the low-intensity side, because it contained 0.005% soluble Ti. Facing this, the authors investigated to which of the soluble and insoluble Ti contents the mode of the nor-

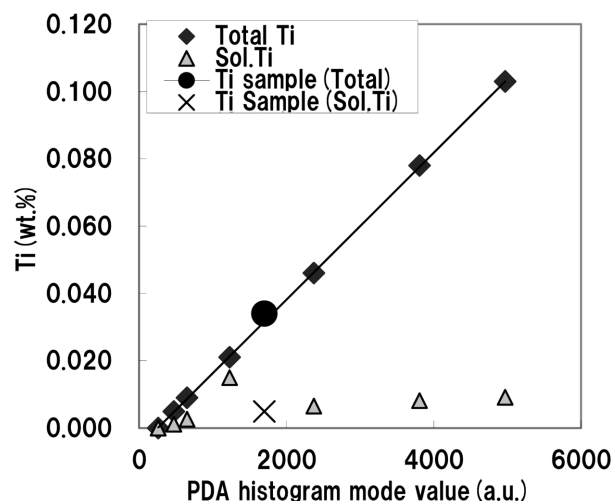


Fig. 3 Relationship between PDA histogram mode value and Total/Sol.Ti

mal distribution portion was proportional.

Fig. 3 shows a plot of the analysis results of the specimens shown in Table 1, the abscissa representing the mode of the normal distribution portions in the PDA histogram and the ordinate, the content of Ti, either total or soluble. The graph demonstrates that the modes of the normal distribution portions are not in proportion to the content of soluble Ti (\blacktriangle) but are in very good proportion to the content of total Ti (\blacklozenge). The analysis result of the Ti sample sat on the straight line of the proportional relationship between the total Ti content and the modes.

It became clear from the above result that the mode value of the normal distribution portion of an element on the low-intensity side of the PDA histogram changed in proportion not to its content in its soluble state only, but to its total content.

3.2 Analysis of breakdown processes of inclusions under spark-OES

The change of a specimen surface under selective spark discharge on inclusions was observed in greater detail in the following four stages: (1) the state of inclusions before spark discharge; (2) the surface condition under selective discharge on inclusions during the initial 10 pulses; (3) the same over 500 pulses at the early stage of stable discharge; and (4) the same over 5000 pulses at the final stage of stable discharge. Table 2 shows the chemical composition of the vacuum-melted Ti specimen (sample No. 8 in Table 1) used for the observation. The specimen surface was finished by belt grinding with #100 polishing paper, and then, without pre-discharge, 10, 500, and 5000 pulses of normal sparks were applied to the specimens.

Fig. 4 shows an intensity-time diagram (IT diagram) of the re-

Table 2 Chemical compositions of Ti sample

wt%	C	Si	Mn	P	Total Ti	Sol.Ti	Al
Ti sample	0.002	0.009	0.20	0.01	0.034	0.005	< 0.002

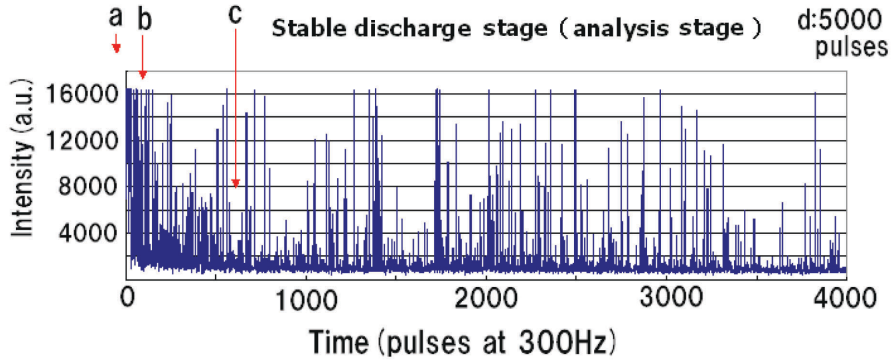


Fig. 4 Spark-OES pulse height spectrum

sults thus obtained; here, the abscissa represents the time, or the number of discharge pulses, and the ordinate represents the emission intensity of Ti. The graph yielded the following findings regarding change in the emission intensity:

- (1) During the initial stage of discharge (roughly up to the 200th pulse), there were very strong spike pulses exceeding the upper sensitivity limit of the device.
- (2) Up to roughly the 500th pulse, the record of which period is disregarded in normal analysis practice as a record of pre-discharge, the discharge intensity decreased gradually, and the fluctuation of the intensity subsided.
- (3) After the above stages of pre-discharge, the fluctuation of emission intensity decreased and the state of discharge entered a stable stage.

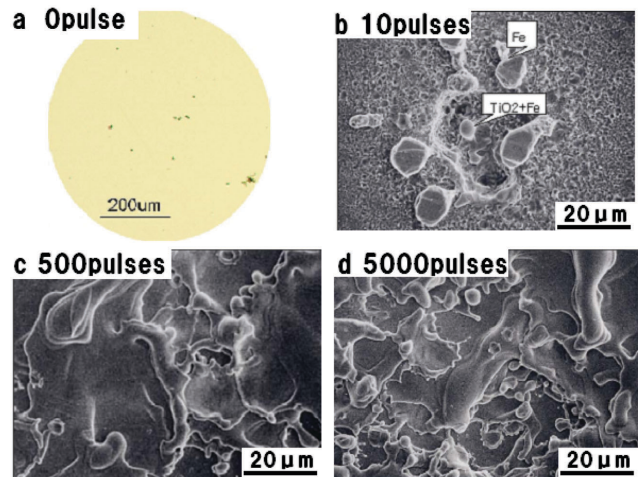
To clarify the reason for the above change in the emission intensity during spark discharge, the authors examined the shape, number, and composition of inclusions at the specimen surface at stages (1) to (4) specified above, using an optical microscope (OM), a scanning electron microscope (SEM), and the EPMA.

3.3 Examination of chronological shape change of inclusions in breakdown processes through OM and SEM

Before OM and SEM observation, to avoid confusion between explosions of alumina abrasive powder due to selective discharge and those of inclusions in the steel, the specimen surface was mirror polished with diamond abrasive instead of alumina. The specimens after mirror polishing were set on the PDA-5500 atomic emission spectrometer, and underwent 10, 500, and 5000 pulses of spark discharge at different positions, and their surfaces were observed before the discharge and after 10, 500 and 5000 pulses through the OM and SEM.

Fig. 5 shows photomicrographs taken through the OM and SEM at different stages. The following findings were obtained from these photographs regarding the breakdown processes of inclusions:

- (1) At stage 1 (before discharge), inclusions were seen as black dots on the surface, Insol. being easily distinguishable from Sol.
- (2) At stage 2 (after 10 pulses), selective discharge on inclusions took place, and the inclusions and the Fe in the matrix were seen to have melted and scattered as fine spherical particles.
- (3) At stage 3 (early stage of stable discharge after 500 pulses) and



(a) Stage 1 (0 pulse), (b) Stage 2 (10 pulses), (c) Stage 3 (500 pulses), (d) Stage 4 (5000 pulses)

Fig. 5 Collapse process of Ti inclusions on the sample surface by spark discharge

stage 4 (final stage of stable discharge after 5000 pulses), rapid melting occurred due to spark discharge and solidification repeated many times, and as a result, there were many spherical objects on the surface. There was no substantial difference between the surface conditions after 500 pulses and the surface conditions after 5000.

To specify the positions of inclusions, some spherical objects suspected to be inclusions were examined using an SEM equipped with an energy-dispersive x-ray spectroscope (SEM-EDS), but none of them were identified as Ti inclusions.

3.4 EPMA examination of chronological shape change of inclusions in breakdown processes

Through observation using the OM and SEM, it could not be clarified whether all Ti inclusions originally exposed at the surface evaporated owing to the selective discharge, or whether they changed their shapes. To solve this problem, the positions where there Ti existed were analyzed through two-dimensional elementary mapping

by EPMA. The measurement was conducted at different positions in grids of 500 by 500 points at a pitch of 1 μm after applying 0, 10, 500, and 5000 pulses of spark discharge, and the intensity ratio between Ti and Fe (total Ti/total Fe) was calculated. In addition, the number of inclusions in the measurement area was counted through image processing.

The EPMA photomicrographs of Fig. 6 showing the breakdown processes of inclusions yielded the following findings:

- (1) At stage 1 (before discharge), hundreds of inclusions were clearly seen at the surface.
- (2) At stage 2 (after 10 pulses), a close examination of the area shown in Fig. 5 (b) disclosed that large inclusions of a Ti system were broken down by selective discharge, and that the inclusions and Fe in the steel matrix melted and solidified into fine spherical particles and scattered around.
- (3) At stage 3 (early stage of stable discharge after 500 pulses) and stage 4 (final stage of stable discharge after 5000 pulses), the number of bright luminous points, supposedly inclusions of a Ti system, fell drastically to less than 10 in a unit area of 500 by 500 μm.

It became clear from the above that a considerable number of inclusions that existed at the surface before the discharge were hit by the sparks and broken down, and that they therefore did not maintain their original shape at the stage of stable discharge after 500 pulses.

Next, to confirm whether the emission intensity of Ti fell significantly as did the number of inclusions at the stage of stable discharge, the authors calculated the emission intensity ratio [total Ti/total Fe] per unit area at different stages.

Fig. 7 shows the result; the abscissa represents the number of discharge pulses (0, 500 and 5000), the ordinate on the left, the relative emission intensity assuming the value of [total Ti/total Fe] before discharge to be 100%, and the ordinate on the right, the number of Ti inclusions found in a unit area of 500 by 500 μm before discharge and after 500 and 5000 pulses. It is clear from the graph that

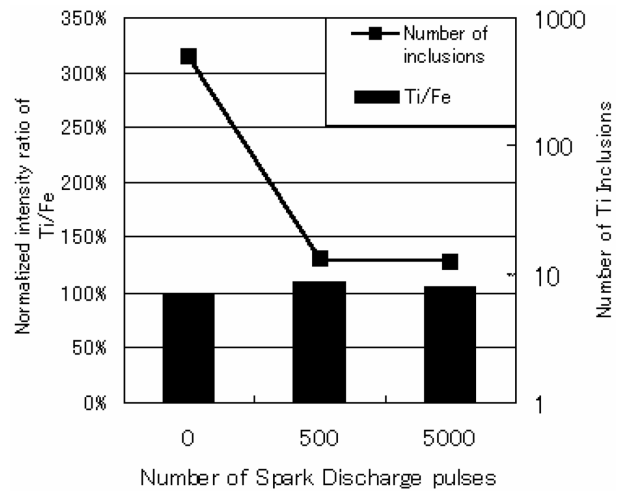


Fig. 7 Relationship between EPMA intensity ratio (Ti/Fe) and number of Ti inclusions

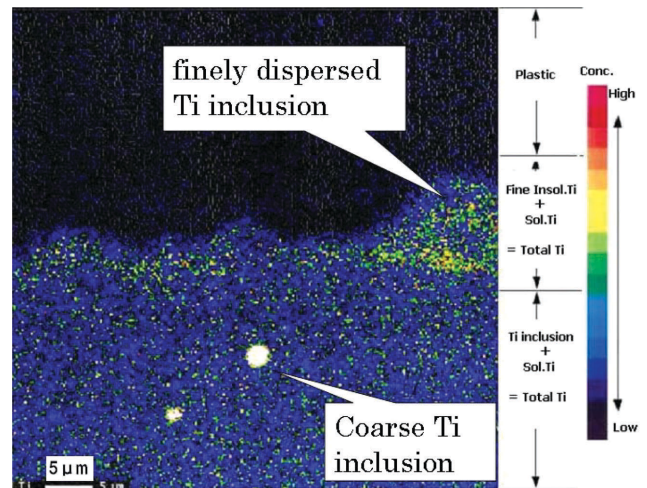


Fig. 8 EPMA mapping of Ti on cross sectional sample surface

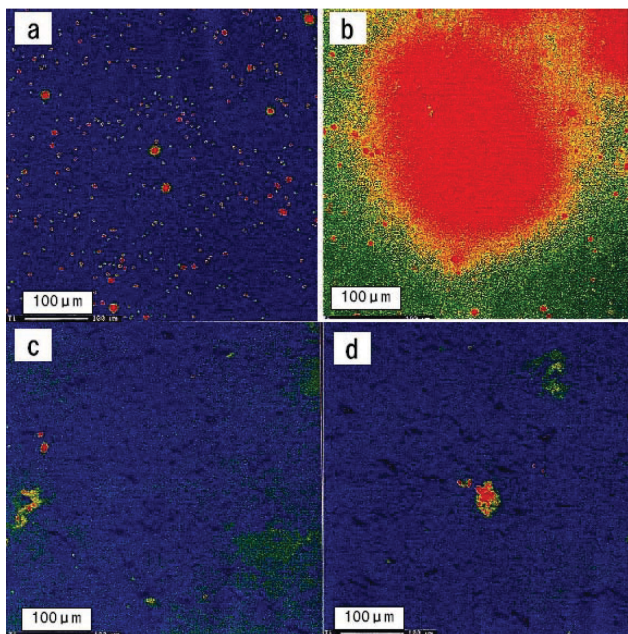
the number of Ti inclusions, which was several hundreds before the discharge, fell to a little more than 10 after 500 and 5000 pulses, but that the emission intensity ratio, which was 100% before discharge, remained substantially unchanged even after 500 and 5000 pulses. The authors presumed from the above that, after being hit by the selective discharge, some of the inclusions were atomized and ionized, contributing to optical emission, and that the rest scattered in the steel matrix as fine particles. To confirm that the inclusions were actually scattered on the specimen surface as fine particles, the surface layer of a specimen was observed at a section using EPMA.

Fig. 8 shows the EPMA mapping of Ti taken at a section of the specimen after 500 pulses. There were spherical Ti inclusions up to several micrometers in size dispersed in the inside of the specimen, which demonstrated that Ti inclusions made finer by the sparks were embedded in the surface layer.

4. Discussion

4.1 Specimen surface model according to conventional PDA theory

Fig. 9 illustrates the theory for distinguishing Sol. from Insol. according to the conventional PDA method. The basic concept of



(a) Stage 1 (0 pulse), (b) Stage 2 (10 pulses), (c) Stage 3 (500 pulses), (d) Stage 4 (5000 pulses)

Fig. 6 EPMA mapping of Ti inclusions before and after spark discharge

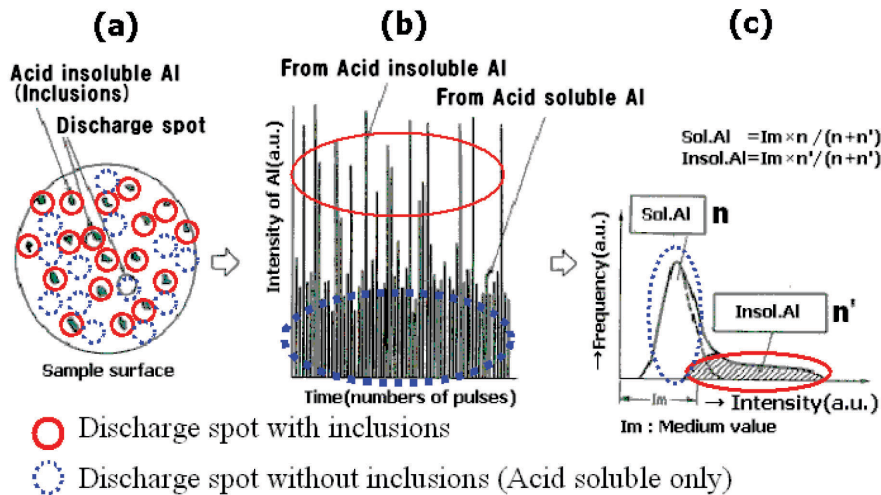


Fig. 9 Principle illustration of PDA method

the determination is as follows: the optical emissions forming a normal distribution pattern on the low-intensity side of the PDA histogram are considered to result from Sol., and those forming the portion stretching to the high-intensity side are considered to result from Insol., and assuming that the ratios of the pulse numbers of the two to the total pulse number are proportional to their respective contents, the amounts of Sol. and Insol. can be defined. This determination method made it possible to clarify the causes of fluctuation in the analysis results intrinsic to spark-OES based on analog integration and to improve the determination accuracy of inclusion-forming elements (Al, S, Ti, Ca, B, etc.) through digital statistical processing, which led to the rapid determination of different substances according to their chemical states.

While selective discharge on inclusions has been known to reveal a wide variety of information about them, according to conventional PDA theory, the optical emissions plotted on a PDA histogram in a normal distribution pattern on the low-intensity side were attributed only to Sol., and those forming the portion stretching to the high-intensity side (red circle in Fig. 9 c), to Insol. such as inclusions. Looking carefully at the schematic illustration of the specimen surface (Fig. 9 a), however, this method of assignment is based on the assumption that inclusions do not break down under sparks at the stable discharge stage, and as a result, soluble and insoluble substances continue to exist separately from each other. This seems to suggest that in conventional explanations of PDA theory, there is a lack of knowledge concerning the change in the specimen surface conditions, or that inclusions at the surface before the spark discharge are broken down by selective discharge by the end of the stable discharge stage.

4.2 Proposal of a specimen surface model at the stable discharge stage of spark-OES

According to the conventional PDA theory of spark-OES, optical emissions forming a normal distribution pattern on the low-intensity side of the PDA histogram are considered to result from Sol., while those forming the portion stretching to the high-intensity side are considered to result from Insol. As the test described in Subsection 3.1 exhibited, however, with PDA histograms of various specimens containing different amounts of Ti, the modes of the normal distribution curves proved to be proportional not to the contents of soluble Ti, but highly proportional to the contents of total Ti.

In addition, as stated in Subsections 3.2 to 3.4, observation of the

breakdown processes of inclusions during spark-OES with OM, SEM, and EPMA made it clear that the schematic illustration of a specimen surface used to explain conventional PDA theory represented the sample surface condition before discharge, and did not correctly reflect the condition at the stage of stable discharge, when analysis data are actually collected. That is to say, before spark discharge, the size of inclusions is close to the diameter of discharge spots, and the inclusions thus emit high-intensity spectrum lines when hit by a spark, but after several hundreds of pulses, most inclusions at the surface have been broken down by selective discharge; it is most likely that some cause optical emission while others disperse in the steel matrix as fine particles as seen in Fig. 8. Then, based on the above test results, the authors attempted to construct a model of a specimen surface at the stage of stable discharge of spark-OES.

Fig. 10 (a) schematically illustrates the conventional PDA model, and (b), the new PDA model that the authors propose. According to the explanations of the conventional PDA model, there are insoluble inclusions of Ti, Al, etc. at the surface of the steel matrix, in which the same inclusion-forming elements also exist in solute state (Sol.), and whereas high-intensity spike peaks are emitted when sparks hit inclusions, low-intensity peaks are emitted forming a normal distribution pattern when sparks hit the matrix (solute portions). This explanation, however, applies only to the state of the specimen surface before spark discharge, and not to the state at the stable discharge stage. What actually happens is that, under spark discharge, inclusions become charged, explode into fine particles giving off spectrum lines of high intensity, and scatter; as a result, surface portions consisting purely of the matrix with solute elements (Sol.) as illustrated in Fig. 10 (a) will no longer exist. The authors instead consider that the model illustrated in Fig. 10 (b), wherein fine insoluble particles of inclusions that have been pulverized and scattered by the sparks are embedded in the surface of the matrix, better reflects the real condition of the sample surface at the stable discharge stage.

When a spark hits the surface in this condition, the optical emission intensity will be the sum of the intensity of Sol. in the matrix and that of the finely scattered insoluble inclusions, and the emission intensity actually recorded will be that of the total content of the element in question (Sol. + Insol.).

If, on the other hand, the surface layer evaporates under the sparks and inclusions in the sub-surface layer become exposed, the newly exposed insoluble inclusions are selectively hit by the sparks and

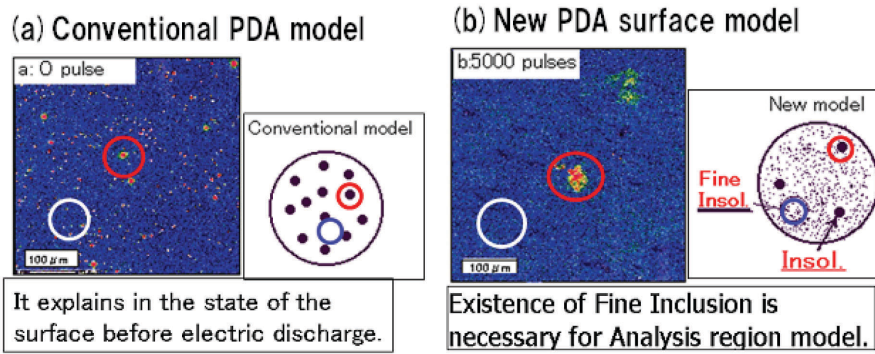


Fig. 10 Comparison of conventional model and proposed model of sample surface at stable discharge stage

high-intensity spectrum lines are recorded, but the frequency of this at the stable discharge stage is far lower than that during the initial several hundreds of pulses.

4.3 Results of re-assignment of PDA histogram patterns

Based on the above test results and discussion, the authors attempted re-assignment of the distribution patterns in PDA histograms.

As explained earlier herein, according to the conventional interpretation of the optical emission of spark-OES, the normal distribution portion on the low-intensity side is assigned to Sol. and the portion distributed on the high-intensity side is assigned to Insol. This manner of assignment, however, is based on the state of existence of inclusions before spark discharge, but in fact, at the stage of stable discharge, most inclusions have been broken down, atomized, ionized, and scattered by selective discharge, and are embedded as extra-fine particles in the matrix. When a spark hits a surface region in this state, the emission intensity of the normal distribution portion will be the sum of that from the original soluble component and that from the scattered fine insoluble particles, corresponding to the total content of the element in question as shown in Fig. 11. For this reason, the normal distribution portion, which has been assigned according to conventional PDA theory to the soluble state of the element in question, must be re-assigned to its total content.

4.4 Relationship between the result of re-assignment of PDA histogram patterns and the high-energy pre-discharge method

In his explanatory work on the history of rapid analysis techniques for steel production, Saeki⁷⁾ reviewed the history of the spark-OES technique, and wrote about the development of the PDA method in 1974. As a typical example of measures to improve the analysis accuracy of spark-OES, he introduced the high-energy pre-discharge method, reported in 1979, that Shibata et al.¹³⁾ developed to improve the determination accuracy of Mn and S in sulfurized free-cutting steel. They maintained that the effects of selective discharge on inclusions could be mitigated by applying pre-discharge with high-energy sparks, because the structure at the specimen surface would be made finer through melting, homogenizing, and rapid cooling. In this regard, the conventional PDA model, which assumes that Sol. and Insol. exist at the specimen surface in a distinctly separate manner, conflicts with the concept of the high-energy pre-discharge method, which assumes that the specimen surface is melted and homogenized.

In addition, in the latest practice of spark-OES, the distribution patterns in PDA histograms are still assigned on the assumption that inclusions at the specimen surface survive the stable discharge stage intact and that Sol. and Insol. exist there separately from each other.^{9, 10, 14, 15)}

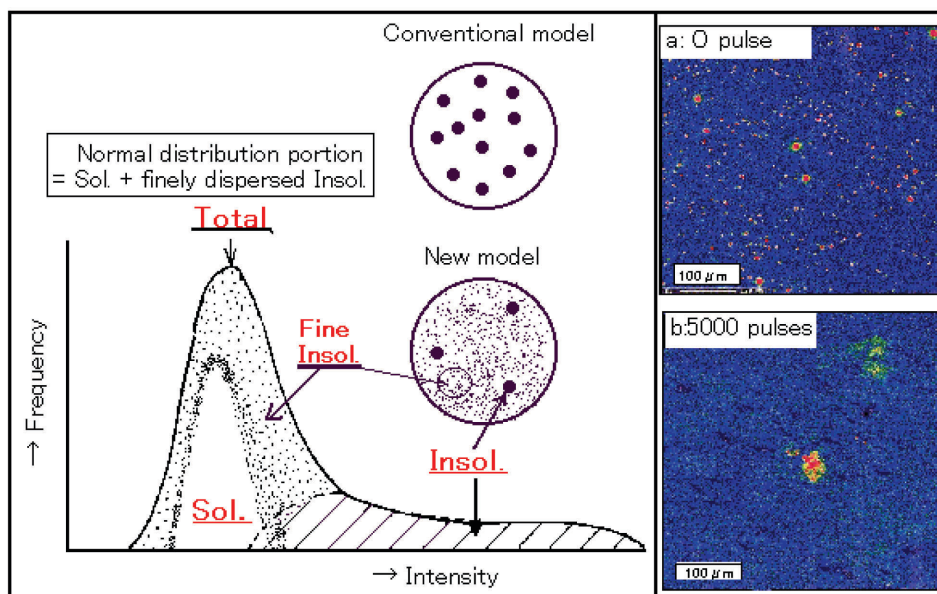


Fig. 11 Reassignment of PDA histogram for Sol., and Insol. components

This means that two contradictory concepts have coexisted in the field of spark-OES of steel materials.

However, as the present report has made clear, most inclusions are broken down, atomized, ionized, and scattered by selective discharge, and are embedded in the matrix as extra-fine particles at the stable discharge stage. When a spark hits a surface region in this state, the intensity of the optical emissions forming the normal distribution pattern in the histogram will be the sum of that from the original Sol. and that from Insol. scattered as fine particles, corresponding to the total content of the element in question. Considering that melting and homogenizing of the specimen surface mitigate the effects of selective discharge on the matrix and inclusions, one can understand the above two major development concepts in an integrated manner as one unified analysis theory.

5. Conclusions

The present study¹⁶⁻¹⁹⁾ aimed to solve a problem in the practice of chemical determination according to conventional PDA theory and to develop a method that enables rapid and accurate determination of components of metal materials according to their chemical states in the refining processes of molten metal. To this end, employing SEM-EDS, EPMA, and spark-OES, the authors examined the breakdown processes of inclusions chronologically at different elementary stages of optical emission in spark-OES, focusing on Ti inclusions in steel as an example. They also conducted tests on the changes in the shape, number, and composition of inclusions from the start of sparks hitting inclusions up to the stage of stable discharge, examined the assignment results based on conventional PDA theory, and, as a result, obtained the following findings:

- (1) The mode of the normal distribution pattern on the low-intensity side of a PDA histogram is proportional not to the soluble content of the element in question in the specimen, but is highly proportional to its total content.
- (2) Before spark discharge, inclusions are clearly identifiable at the specimen surface, but by the stable discharge stage, they have been broken down after being hit by the sparks and do not maintain a definite shape.
- (3) On the other hand, from EPMA results, the relative intensity [total Ti/total Fe] remains substantially unchanged after 500 and 5000 pulses compared to that before spark discharge.
- (4) After being hit by discharge sparks, some inclusions at the specimen surface ionize and atomize, contributing to optical emission, while the rest of them are scattered as fine particles over the matrix.
- (5) When a spark hits a matrix portion where inclusions are scattered as fine particles, the resulting curve in normal distribution

in the PDA histogram reflects the emission intensity from the original Sol. plus that from Insol. scattered as fine particles, namely the intensity corresponding to the total content of the element in question.

- (6) It follows, therefore, that the normal distribution curve in a PDA histogram that was assigned to Sol. according to conventional PDA theory should be re-assigned to the total content (Sol. + Insol.) of the element in question.
- (7) The two distinct development trends in the field of spark-OES, namely the PDA method and the high-energy pre-discharge method, can be understood as one unified analysis theory.

The above findings are applicable not only to the Fe-Ti system but also to a wider variety of metal materials, and as such, add new knowledge to the PDA practice for spark-OES, contributing to the enhancement of the analysis accuracy of the method.

References

- 1) Onodera, M., Saeki, K., Nishizaka, T., Sakata, J., Ono, I., Fukui, I., Imamura, N.: *Tetsu-to-Hagané*. 60, 2002 (1974)
- 2) Imamura, N., Fukui, I., Ono, J., Onodera, M., Saeki, M.: 1976 Pittsburgh Conference on Analytical Chemistry and Applied Spectroscopy. Paper Number 42, 1976
- 3) Ono, J., Saeki, M.: *Bunseki (J. of the Japan Society of Analytical Chemistry)*. (6), 430 (1985)
- 4) Ono, J., Fukui, I., Imamura, N.: *Shimadzu Review*. 35, 1/2, 15 (1978)
- 5) Kamata, H.: *The Latest Analysis Techniques for Steel*. AGNE Gijyutsu Center, Tokyo, 1979, p. 107
- 6) *Analytical Control of Iron and Steel Making in Japan*, Edited by the Committee on Steel Analysis, Iron & Steel Institute of Japan, Tokyo, 1982, p. 506
- 7) Saeki, M.: *Rapid Analysis of Steel Chemistry—Aiming for Speed, Accuracy, and Reliability*. Chijin Shokan Co., Ltd., Tokyo, 1998, p. 95
- 8) Wagatsuma, K.: *Advanced Technologies of Iron and Steel Analysis*. Proceedings of 55th Shiraishi Memorial Technical Conference. ISIJ, Tokyo, 2004, p. 17
- 9) Kuss, H., Lungen, S., Muller, G., Thurmann, U.: *Anal Bioanal. Chem.* 374, 1242 (2002)
- 10) Kuss, H., Mittelstaedt, H., Mueller, G.: *J. Anal. At. Spectrom.* 20, 730 (2005)
- 11) Narita, K., Hara, H., Tokuda, T., Morita, S., Nonomura, E., Narita, T.: *Jpn. Inst. Met.* 43, 1036 (1979)
- 12) Yamaji, M., Hiramatsu, S., Watanabe, T., Fukui, I., Yuasa, S., Omori, T.: *CAMP-ISIJ*. 3, 601 (1990)
- 13) Shibata, T., Hamada, S., Okuyama, Y., Kashiwao, Y., Ono, A.: *Bunseki Kagaku*. 33, 491 (1984)
- 14) Falk, H., Wintjens, P.: *Spectrochimica Acta. Part B* 53. 49 (1998)
- 15) Meilland, R., Dosdat, L.: *Rev. Metall. Cah. Inf. Tech.* 99 (4), 373 (2002)
- 16) Mizukami, K., Ohashi, W., Sasai, K.: *CAMP-ISIJ*. 17, 536 (2004)
- 17) Mizukami, K., Ohashi, W., Sasai, K.: *CAMP-ISIJ*. 17, 1464 (2004)
- 18) Mizukami, K., Mizuno, K., Ohashi, W., Sugiyama, M., Tsuji, M.: *Proceedings of Asia Steel Int. Conf.* 11D-16, 860 (2006)
- 19) Mizukami, K., Sugiyama, M., Ohashi, W., Mizuno, K., Tsuji, M.: *Tetsu-to-Hagané*. 93, 583 (2007)



Kazumi MIZUKAMI
Chief Researcher, D.Eng.,
Materials Characterization Research Lab.,
Advanced Technology Research Laboratories
20-1, Shintomi, Futtsu, Chiba



Masaaki SUGIYAMA
Chief Researcher, D.Eng.,
Materials Characterization Research Lab.,
Advanced Technology Research Laboratories



Wataru OHASHI
General Manager, Ph.D.,
Ceramics & Metals Research Lab.,
Advanced Technology Research Laboratories



Kaoru MIZUNO
Research Center,
Nippon Steel Techno Research



Masaharu TSUJI
Professor of the Laboratory of Heterogeneous Inte-
grated Materials, Department of Integrated Materials
Institute for Materials Chemistry and Engineering,
Kyushu University